JOURNAL OF GEOPHYSICAL RESEARCH, VOL. 106, NO. D22, PAGES 28,427-28,439, NOVEMBER 27, 2001

Large-scale advection of continental aerosols during INDOEX

J.-F. Leon,[1] P. Chazette,[1] F. Dulac,[1] J. Pelon,[2] C. Flamant,[2] M. Bonazzola,[3]
G. Foret,[4] S. C. Alfaro,[5] H. Cachier,[1] S. Cautenet,[4] E. Hamonou,[1]
A. Gaudichet,[5] L. Gomes,[5] J.-L. Rajot,[5] F. Lavenu,[6] S. R. Inamdar,[7]
P. R. Sarode,[8] and J. S. Kadadevarmath[7]

Abstract. In this paper, we present passive and active remote sensing measurements of atmospheric aerosols over the North Indian Ocean (NIO) during the Intensive Field Phase (IFP, January to March 1999) of the Indian Ocean Experiment. The variability of the aerosol load over NIO is discussed based on three-dimentional numerical simulations made at a local scale by use of Regional Atmospheric Modeling System (RAMS) and at a regional scale using the zoomed Laboratoire de Météorologie Dynamique global circulation model (LMD-Z version 3.3). Ground-based measurements of the columnar aerosol optical thickness (AOT) and of surface black carbon (BC) concentration were carried out at two different sites in India: Goa University on the NIO coast and Dharwar 150 km inland. Local-scale investigations point out that the trend in BC concentration at the ground is not correlated with AOT. Lidar profiles obtained both from the surface at Goa and in the NIO from the Mystere-20 research aircraft indicate that a significant contribution to the total AOT (more than 50%) is due to a turbid monsoon layer located between 1 and 3 km height. RAMS simulation shows that the advection of aerosols in the monsoon layer is due to the conjunction of land-sea breeze and topography. We present the regional-scale extent of the aerosol plume in terms of AOT derived from the visible channel of Meteosat-5. During March, most of the Bay of Bengal is overcast by a haze with a monthly average AOT of 0.61±0.18, and a spatially well-defined aerosol plume is spreading from the Indian west coast to the Intertropical Convergence Zone with an average AOT of 0.49±0.08. Those values are bigger than in February with AOT at 0.35±0.18 and 0.37±0.09 for the Bay of Bengal and the Arabian Sea, respectively. One of the principal findings of this paper is that a significant contribution to the aerosol load over the NIO is due to the advection of continental aerosols from India in a well-identified monsoon layer above the marine boundary layer. Moreover, it is suggested that the increase in biomass burning plays a significant role in the increasing trend in AOT during the winter dry monsoon season.

[1]Laboratoire des Sciences du Climat et de l'Environnement, CEA-CNRS, Gif-sur-Yvette, France.

[2]Service d'Aéronomie, CNRS Paris, France.

[3]Laboratoire de Météorologie Dynamique, CNRS, Paris, France.

[4]Laboratoire de Météorologie Physique, CNRS-Université Blaise Pascal, Clermont-Ferrand, France.

[5]Laboratoire Inter-universitaire des Systèmes Atmosphériques, CNRS-Université PVII/PXII, Créteil, France.

[6]Centre d'Etude Spatiale de la Biosphère, Centre National d'Etudes Spatiales, Toulouse, France.

[7]Department of Physics, Karnataka University, Dharwar, India.

[8]Department of Physics, Goa University, Goa, India.

Paper number 2001JD900023.
0148-0227/01/2001JD900023$09.00

1. Introduction

Assessing the radiative forcing of tropospheric aerosols is a challenge due to the high spatial and temporal variability of their physical, chemical and optical properties [*Intergovernmental Panel on Climate Change*, 1995]. Industrial and urban emissions are a major source of aerosols which are recognized to be of paramount importance in the Earth's radiative budget because of their both optical [*Charlson et al.*, 1992; *Boucher and Anderson*, 1995] and cloud condensation properties [*Twomey*, 1974]. They also act on the photochemistry of the troposphere [*Andreae and Crutzen*, 1997; *Dickerson et al.*, 1997]. Anthropogenic aerosols are composed of a complex mixture of primary solids, such as mineral dust and graphitic carbon, and water-soluble particles such as sulfates, ni-

trates, and organic matter [*Warneck*, 1988]. Estimating the climate forcing of tropospheric aerosols requires the knowledge of the spatial distribution of the particles and their optical and cloud-nucleating properties. The Indian Ocean Experiment (INDOEX) [*Ramanathan et al.*, 1995] aims at quantifying the radiative effect of anthropogenic aerosols over the North Indian Ocean (NIO), with special emphasis on the apportionment of each constituent of the mixture to the radiative impact and the spatial extent of this impact.

During the winter (dry) monsoon, anthropogenic aerosols are advected by predominant northeasterly winds from the Indian subcontinent to the Indian Ocean. *Satheesh et al.* [1998] have measured a spatial gradient of aerosol optical thickness from the Indian coast to the open ocean mainly corresponding to a decrease in the columnar mass loading rather than a change in the optical properties, which suggests a long-range transport and dilution of continental aerosols over the NIO. These aerosol plume observations have been confirmed off the Indian coast, between Bombay and Goa, from the measurements of the spaceborne POLDER instrument [*Deuzé et al.*, 1999] during 1996-1997 winter. Following these observations, the main INDOEX intensive field phase (IFP) occurred between January and March 1999 [*Coakley et al.*, 2001]. Our strategy was to complete aerosol observations over the NIO performed during IFP by in situ measurements in India. In this paper we present the optical measurements performed at two sites in Southern India, Meteosat-5 satellite analysis of the aerosol content over the ocean and three-dimentional (3-D) model simulations with the aim of studying processes responsible for the large-scale advection of continental aerosols.

Instrumental setup and mesoscale and synoptic models used for the data interpretation will be presented in section 2. Section 3 will be devoted to the interpretation of local-scale aerosol measurements, whereas section 4 focuses on the regional extent of the aerosol plume during the IFP.

2. Experimental Setup and Numerical Transport Models

Two ground-based stations were operated during the IFP at both the Goa University (15°45'N, 73°8'E, hereafter referred as Goa) and the Karnataka University (15°42'N, 74°98'E, hereafter referred as Dharwar). As shown in Plate 1, the Goa experimental site is bounded at its western side by the Arabian Sea and by the Western Ghats at its eastern side. The Western Ghats are a 700 m high mountain range, parallel to the seashore and located at about 50 km from the Goa site. Onto the Western Ghats, Dharwar is located 150 km east from Goa. Since Goa is roughly downwind of Dharwar with respect to the dominant northeasterly winds prevailing in this area during the winter monsoon, one can expect to assess the evolution of the aerosol properties during their transport. In situ instruments as well as active and passive ground and spaceborne remote sensors have

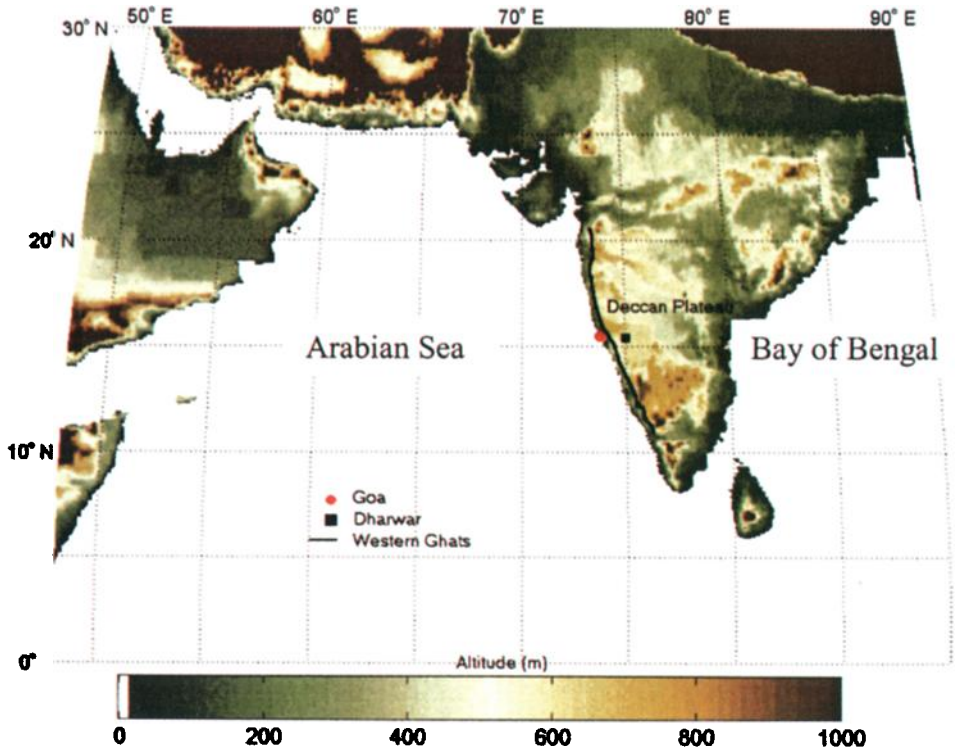

Plate 1. Location of the ground-based stations operated during IFP 99. Positions are plotted on a digital elevation model map (in meters).

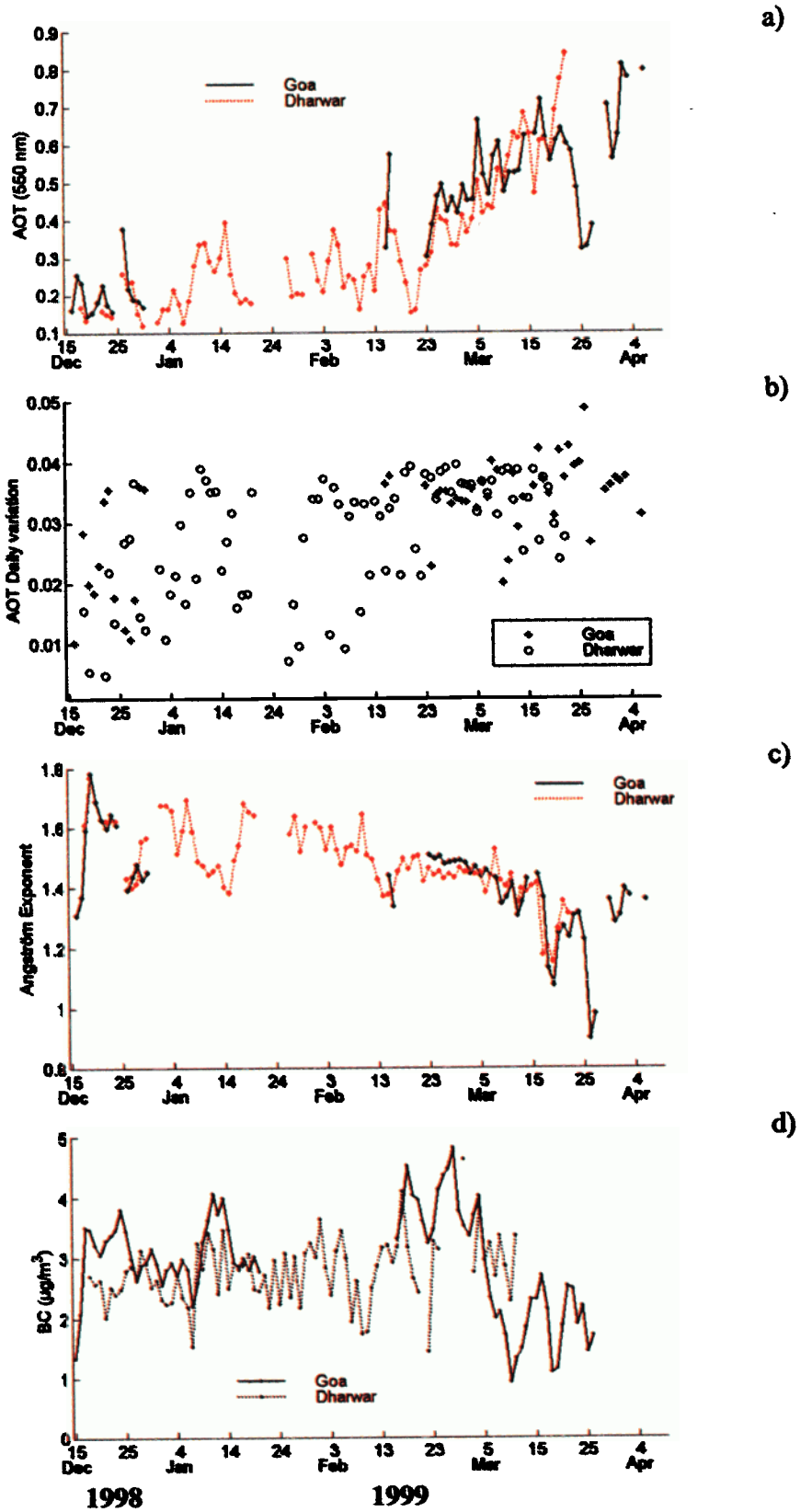

Plate 2. Daily mean (a) AOT at 550 nm and (c) AE derived from automatic Sun tracking photometer from December 1998 to April 1999 at Goa (solid line) and Dharwar (dashed line). (b) AOT daily standard deviation from December 1998 to April 1999 at Goa (stars) Dharwar (circle). (d) Mean daily BC concentration recorded at Goa (solid line) and Dharwar (dashed line).

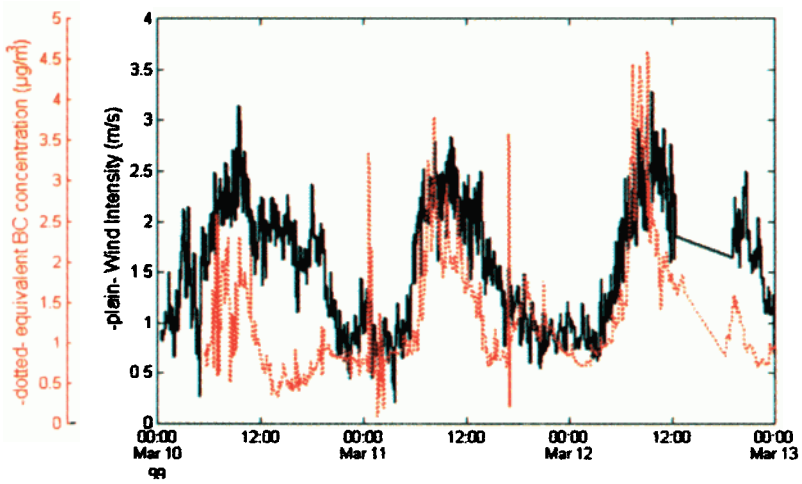

Plate 3. Zoom of the BC concentration daily variation (recorded every 10 min) between March 10 and 13, 1999, at Goa. The wind speed at 10 m is also displayed.

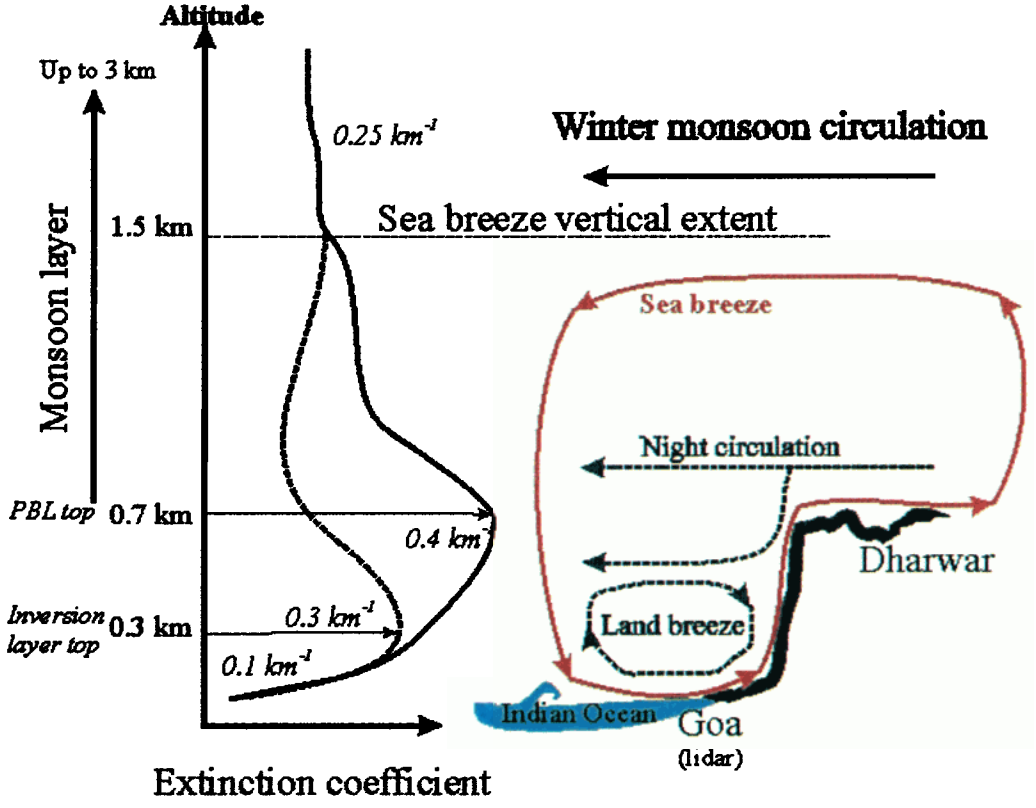

Plate 4. Schematic representation of a zonal cross section between Goa and Dharwar of the atmospheric circulation onto the Western Ghats. The mean aerosol extinction coefficient (in km^{-1}) derived from micropulse lidar measurements is displayed at the left side of the figure as a function of the altitude. Solid line represents daytime measurements, and dotted line is for nighttime conditions.

been involved in our experimental setup. Both synoptic and mesoscale transport models have been used for the data interpretation.

2.1. Experimental Data Set

At Goa, both size distributions and chemical composition were measured during March 1999 by means of particle size counters, filter sampling analysis and black carbon concentration measurements by means of an aethalometer. Moreover, a ground-based lidar and an automatic Sun tracking photometer were also deployed. The Dharwar station was equipped with an automatic Sun tracking photometer and an aethalometer.

2.1.1. Integrated columnar measurements. Automatic Sun tracking photometer instruments [*Holben et al.*, 1998] manufactured by CIMEL Electronics, operated at Goa and Dharwar. The incoming spectral radiance of the direct solar beam radiation was measured at four wavelengths: 440, 670, 870, and 1020 nm. The aerosol optical thickness (AOT) was retrieved based on a careful instrument calibration performed following the method developed by *Herman et al.* [1981]. The relative error on the retrieved AOT remains less than 5% for an AOT closed to 0.4 [*Fouquart et al.*, 1987; *Tanré et al.*, 1988; *Hamonou et al.*, 1999]. From spectral AOT measurements at 440 and 670 nm, the visible Ansgtröm exponent [*Angström*, 1964] has been derived with a relative error less than 10% at the encountered optical thickness [*Hamonou et al.*, 1999].

The Sun photometer operated from December 16, 1998, to April, 5, 1999 at Goa with only 2 days of measurements between January 1 and February 25, 1999, due to a failure. At Dharwar the sun photometer operated continuously from December 18, to March 24.

2.1.2. Ground sampling measurements. Black carbon (BC) is defined as the light-absorbing component of carbonaceous aerosols. BC is an indicator of air masses affected by anthropogenic pollution [*Penner*, 1995]. During the IFP we have monitored BC equivalent concentration by use of two aethalometers (model AE14, Magee Scientific) operating at Dharwar and Goa. The measurements have been calibrated with the protocol defined by *Ruellan and Cachier* [2001]. The residual relative error established by these authors is close to 10%.

At the coastal site the record starts mid-December until the end of March, but due to a failure in the pumping system, a break occurred between January 21 and February 15. At the inland site a continuous record is available from mid-December till mid-March.

2.1.3. Ground and airborne columnar lidar measurements. From March 1 to 15 we operated a monochromatic (523 nm) micropulse lidar [*Spinhirne*, 1993] at the Goa station. Vertical profiles were acquired during nighttime and daytime. Lidar LEANDRE-1 [*Pelon et al.*, 1990] on board the French research aircraft Mystere20 has acquired aerosol backscatter vertical profiles along a path coming from Kashidoo (4.2°N, 73.6°E, Maldives Republic) to a point in the Arabian Sea located at 8.5°N and 71°E on March 8. From those two observations one can expect to have a description of the aerosol vertical extent from the coast to the open ocean.

Solving the lidar equation (to obtain extinction profile) requires the knowledge of a boundary condition taken in the form of a reference backscatter coefficient value and the profile of the ratio of the aerosol backscatter coefficient to the extinction coefficient [*Klett*, 1983]. The sensitivity of the retrieved extinction coefficient profile to the input parameter is described by *Chazette et al.* [1995]. For the ground-based lidar the boundary condition is taken at the far end of the range at an altitude above 4 km, and for the airborne lidar the boundary condition is taken near the plane ($\approx$ 7 km). In both cases the boundary condition corresponds to Rayleigh scattering. The value of the backscatter to extinction ratio is taken constant with altitude and equal to 0.012 sr^{-1} [*Chazette et al.*, 2000]. This value has been obtained by comparison between LEANDRE-1 lidar integrated derived extinction profiles near Male and aerosol optical depth measured with a Sun photometer at Male observatory. Moreover this value is consistent with Mie calculation performed using the aerosol model derived at Goa for a mean relative humidity of 70%. We assume that this value is also relevant for the inversion of lidar profile measured at the Goa University. The relative possible bias on the total extinction due to the a priori knowledge of the aerosol model is less than 20%.

2.1.4. Regional satellite observations. During the IFP, thanks to the shift of the European geostationary satellite Meteosat-5, a daily monitoring of AOT by analysis of the visible channel was possible. We have used NetCDF low-resolution visible channel data files provided by the Laboratoire de Météorologie Dynamique (LMD, Palaiseau, France). Images are projected on a regular latitude-longitude grid with a resolution of 0.25° which corresponds to a sample of 10x10 full resolution pixels. Numerical counts, 3×3 and 10×10 neighborhood standard deviation of the original central pixel, are stored in the file.

Moulin et al. [1997a, 1997b] describe an algorithm for long-term monitoring of Saharan dust load over both North Atlantic and Mediterranean using the visible channel (VIS) of successive satellites of the Meteosat series. The processing scheme which is applied in this section is based on the same protocol, adequate over low-albedo surfaces (ocean surfaces only). It is as follows: (1) data preprocessing including cloud detection and masking, masking of the Sun specular reflection on water surface, and digital count transformation to radiance values; (2) inversion of measured radiance value to AOT based on a look-up table (LUT) scheme over open ocean (clear water). The conversion of numerical count into radiance value is done using calibration coefficient provided by Eumetsat [*Govaerts et al.*, 1998].

To avoid glitter contamination, a mask is applied for angles within 40° of the glitter angle. To obtain a significant amount of off-glitter pixel and then to derive a daily monitoring of AOT, it was necessary to used a synthesis of several Meteosat acquisition during the day: 6 hourly slots from 0600 to 1100 UT were thus considered and averaged to provide a daily map of AOT.

We have completed our data set with observation of the number of fires in India derived from the Along Track Scanning Radiometer (ATSR) World Fire Atlas [*Arino*, 1997]. The algorithm is based on the saturation of the 3.7 μm ATSR-2 channel at nighttime. Data are available at http://shark1.esrin.esa.it/ionia/FIRE/.

2.2. Numerical Approach

2.2.1. Mesoscale modeling. The particular location of the two ground-based stations requires to have a good knowledge of the atmospheric circulation taking into account the effect of land-sea breeze as well as the effect of the topography. For this purpose, we have used the Regional Atmospheric Modeling System (RAMS) [*Mahrer and Pielke*, 1978]. The initialization is obtained from the 00 UT European Centre for Medium-Range Weather Forecast (ECMWF) data. A weak nudging of meteorological fields is carried out every 6 hours. We consider simulations between 00 UT on March 4 and 2400 UT on March 5. The domain is bounded between 73°E and 76°E in longitude, and 16°N and 14°N in latitude. This domain consists in 120 grid points in the zonal-direction and 80 grid points in the meridian-direction. The horizontal grid spacing is 3 km in both east-west and north-south directions with 30 sigma-z levels. The vertical grid spacing is 25 m near the ground with a geometric stretch ratio of 1.2 and a maximum interval of 1000 m above 3000 m up to the model top at 15.6 km high. The geometric stretch ratio is used to provide a higher resolution close to the ground. The time step is 20 s. The topography is taken from the National Oceanic and Atmospheric Administration web site – http://www.ngdc.noaa.gov/seg/topo/. Sea surface temperatures are obtained from ECMWF database. The cover vegetation (forest, agricultural areas) is taken into account. This heterogeneous surface is very important to correctly simulate the breeze winds [*Kikuchi et al.*, 1981; *Ookouchi and Wakata*, 1984]. Two tracers are emitted every 3 hours, one from Goa near the coast and the other from Dharwar on the plateau, and are transported.

2.2.2. Synoptic meteorological fields. Synoptic meteorological conditions are derived from the ECMWF data available from the Laboratoire de Météorologie Dynamique. Those data are restricted to the INDOEX geographical area (35°N to 35°S and 30°E to 110°E) and provided on a regular latitude-longitude grid of 0.5°×0.5° over standard pressure levels. Wind direction and speed as well as relative humidity fields have been considered.

2.2.3. Synoptic modeling. To describe air mass advection at the regional scale over the ground-based station, we have performed air mass reverse transport computations using the Laboratoire de Météorologie Dynamique global circulation model Zoomed version 3.3 (LMDZ.3.3) following the method described by *Hourdin and Issartel* [2000]. This method is based on the time symmetry of the transport equation and on this point does not differ from lagrangian back tracking [*Hess et al.*, 1996] that only takes into account large-scale transport. The same method is used to simulate other transport processes such as turbulent and convective mixing as well as linear sinks (modeled by means of an exponential decay with a time constant of 7 days). The model is used at 1.2°×1.2° horizontal resolution by coordinate stretching and with a hybrid σ-pressure vertical coordinate over 19 levels.

3. Local-Scale Investigation

3.1. Surface and Column-Integrated Observations

Daily mean AOT at 550 nm derived from Sun photometer measurements performed at Goa and Dharwar are plotted on Plate 2a as a function of time from mid-December 1998 to the beginning of April 1999. For both sites the temporal trend in the AOT is very similar. AOT measured at Dharwar (the most representative with 83 days of acquisition compared to 54 for the Goa site) increases from 0.16 to 0.83 from mid December 1998 to the end of March 1999. The average rate of increase in AOT from mid-December 1998 to the end of February 1999 is 0.002 per day while during March, this rate is one order of magnitude higher. For most of the period, AOT measured at Goa and at Dharwar are very similar with an average difference of ±0.07. The daily variability of the AOT is shown in Plate 2b. Low daily AOT amplitudes (less than ±0.04) highlight that the AOT is not affected by the variation of local sources such as car traffic or domestic fire and thus must be representative of an aerosol load associated with a large scale transport.

As for the AOT, the trend in the visible Angström exponent (AE, which indicates the spectral dependence of AOT) shown in Plate 2c, is very similar for both sites. AE values depends mostly on the aerosol size distribution and complex refractive index. For submicron particles such as sulfates or carbonaceous aerosols, a typical AE value is between 1 and 2 [*Liousse et al.*, 1995]. One can observe a slight decrease in the AE from 1.6 to 1.3 (±0.2) from December to end of March. The nearly constant value of the AE until mid-February indicates that the aerosol optical properties are not changing significantly and we can interpret the increase in the AOT as an increase in the columnar aerosol load. The fast increase in AOT observed in late February is associated with a slight decrease in AE which indicates a change

in both the columnar aerosol load and the aerosol optical properties. For AOT less than 0.2, AE values could be associated with important errors [*Hamonou et al.*, 1999] and their temporal variability could be significantly affected increasing the spread. Nevertheless, the minimum (0.9-0.95) observed on March 25 and 26 is significant and is likely associated to a mineral dust plume advected over the site. This hypothesis is discuss in the last section of this paper. The decrease in AOT from 0.6 to 0.3 seems to indicate that this air mass advection disturbs the monsoon flow.

The mean daily ground BC concentrations recorded at the twin sites from mid-December 1998 to late March 1999 are shown on Plate 2d. As for the column AOT, higher surface concentrations are observed at the coastal site. Until late February, a weak temporal behaviour is observed for both sites. The mean daily BC concentration remains quite constant from mid-December to mid-February, about 3 ± 0.7 μgm^{-3}, at the coastal site. An increase in the BC concentration is recorded at both sites in late February. This increase is simultaneous with the increase in the AOT and then should indicate an increase in the columnar aerosol load. The BC concentration recorded at Goa starts to decrease in early March ($\approx 1.5\pm0.7\mu gm^{-3}$) while the Sun photometer measured-AOT is still increasing (Plate 2a). The BC concentration recorded at Dharwar is the same as in late February ($\approx 3\mu gm^{-3}$).

The BC concentration depends strongly on the time of the day as opposite to the AOT. A daily variation of BC concentration and meteorological parameters due to the effect of land-sea breeze is observed at the station. The daily variation of BC concentration and wind intensity recorded on a meteorological mast at the station is illustrated on Plate 3 between March 10 and 13.

3.2. Dynamical Processes

We analyze the daily variation using a mesoscale model accounting for the sea breeze and the catabatic winds effects associated to the topography between the two instrumented sites. A scheme of the nighttime and daytime dynamics highlighted by the model is given in Plate 4 (right side) which represents a schematic zonal cross section of the atmospheric circulation between the two sites. The mean daytime and nighttime vertical profiles of aerosol extinction coefficient derived from the lidar are also presented (Plate 4, left side).

The daytime atmospheric circulation corresponds to a sea breeze circulation inside the winter monsoon flow. In the afternoon, below 1000 m in altitude, we have an intense sea breeze enhanced by the topography [*Kikuchi et al.*, 1981], with an intrusion across the plateau as far as Dharwar in the afternoon, that is to say a distance of $\approx$ 150 km from the coast. The updrafts connected to breeze circulation allow pollutants to reach up to 2.5 km in altitude, so that the aerosols are able to be transported in the free troposphere by the winter monsoon flow. At Goa, the mean altitude of the daily planetary boundary layer have been found close to 0.7 km during all the measurement period (Plate 4, left side). At Dharwar in the afternoon, the local dry convection linked to strong instability raises the pollutants, but the ascent is very important when the sea breeze front arrives. A strong convergence develops because the sea breeze meets the winter monsoon. The Goa and Dharwar plumes can mix above the plateau in the late afternoon. The efficiency of the sea breeze is then increased by the catabatic winds induced by the topography which may conduct to homogenize the atmospheric column between the two sites as indicated by the coherence between Sun photometer measurements at Goa and Dharwar (Plate 2a and 2b). The ascension of air masses on the Deccan plateau implies that the advection of pollutant from the Indian subcontinent over the NIO occurs significantly over the marine boundary layer. It is verified by lidar profiles performed both from the Goa ground-based station (Plate 4, left side) and the Mystere20 research aircraft $\approx$1000 km offshore Indian coast (Figure 1). Indeed, for both observations the monsoon layer is located between $\approx$ 1 to 3 km high with a mean extinction coefficient close to 0.25 km^{-1}.

On the other hand during nighttime, the land breeze associated with a weak vertical development (nocturnal stability) in altitude (300 m) keeps the pollutants near the source and close to the ground. This is confirmed by lidar sounding at Goa highlighting an inversion layer top close to 0.3 km (Plate 4, left side)

Over the whole micropulse lidar operating period (March, 1-14, 1999), we computed the ratio of AOT obtained by integration of extinction coefficient vertical profiles from 1 to 3 km to the total AOT. Results are plotted in Figure 2. This ratio ranges between 45 and 70% with an increasing trend during the second half of the operating period. On Figure 1, the accumulated AOT between the top of the atmosphere and the given altitude is plotted as a function of the altitude. This ratio is $\approx$ 53.5% for the profile displayed on Figure 1. This observation confirms that most of the pollutants from the Indian subcontinent are transported over the marine boundary layer up to 3 km height allowing a long distance transport by the NE winds. Thus the increase in AOT during March observed at the Goa station from Sun photometer measurements seems to be linked to a regional change of the aerosol load above the marine boundary layer.

4. Regional-Scale Extent

4.1. Satellite Observations

The AOT retrieval from Meteosat needs an assumption on the aerosol optical characteristics, i.e., the phase function and the single scattering albedo, to compute

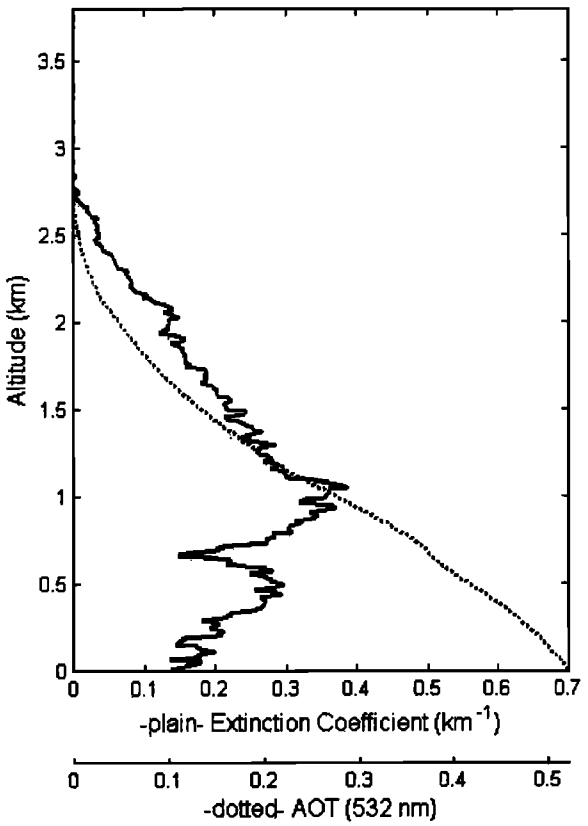

Figure 1. Profile of the aerosol extinction coefficient (solid line) measured in the NIO (8.5°N; 71°E) by the lidar Leandre-1 on board Mystere-20 research aircraft on March 8, 1999. The dotted line represents the accumulated AOT corresponding to the integration of the aerosol extinction profile between the top of the atmosphere and the given altitude.

the LUT. Following previous observations in the NIO [e.g. *Moorthy et al.*, 1998; *Satheesh et al.*, 1998; *Chazette et al.*, 2000], pointing out the predominance of the accumulation mode with a 0.06 μm mean number radius (standard deviation of 1.72), we have used this value

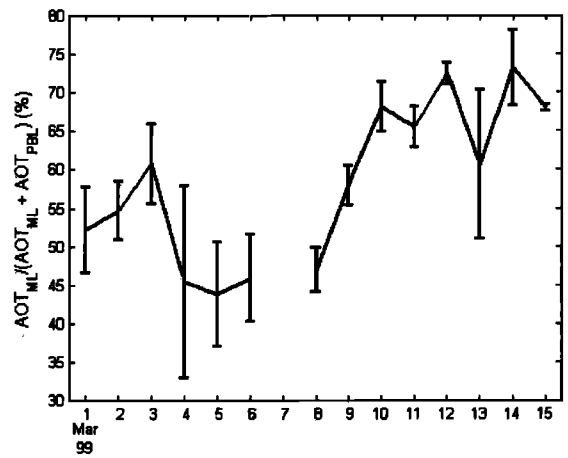

Figure 2. Ratio of the lidar-derived AOT integrated between 1 and 3 km height to the total AOT as a function of the day. The vertical bars represent the associated daily range of variation.

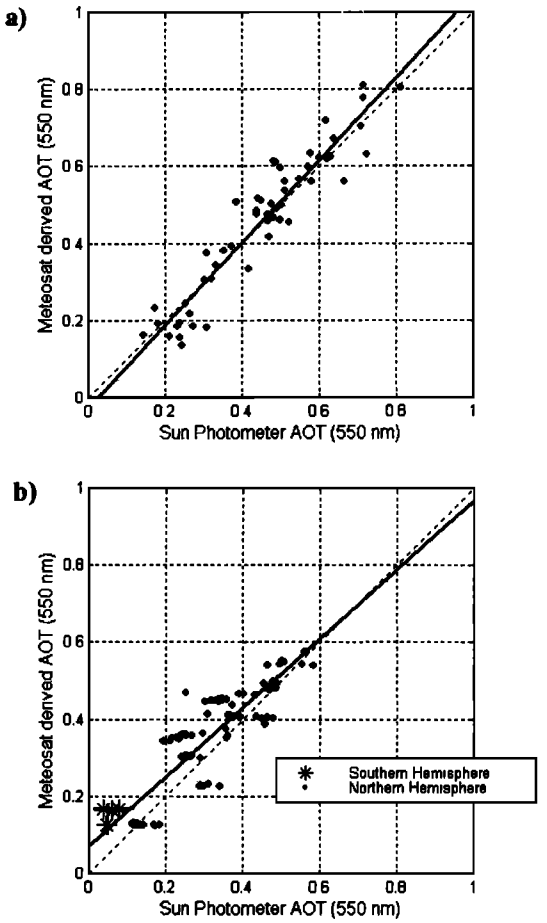

Figure 3. (a) Comparison between Sun photometer AOT measured at the Goa experimental site and Meteosat-5 derived AOT. Meteosat pixels within a range of 100 km from the ground-based station are selected and averaged. (b) Comparaison between Sun photometer AOT measured on board RV Sagar Kanya (courtesy of A. Jayaraman) and Meteosat-5 derived AOT.

to compute the LUT. The aerosol refractive index was then adjusted to best fit ground-based Sun photometer measurements performed at Goa (Figure 3a). The fitted value of 1.43-i0.03 has been found to be in a good agreement with the value derived from ground-based studies. We have also compared this equivalent AOT with the set of data obtained onboard Indian research vessel *Sagar Kanya* (available at http://joule.oce.orst.edu/aerosol) [see also *Jayaraman et al.*, 1998] and the result is displayed on Figure 3b pointing out the agreement between surface observations and our satellite product.

The increase in AOT observed at Goa and Dharwar in March compared to February (Plate 2a) is not just a local phenomenon. Plate 5 presents the average Meteosat-5 derived AOT for the last 10 days of February 1999 (Plate 5a) and the three periods of 10 days of March 1999 (Plate 5b, 5c and 5d). White areas correspond to missing data due to clouds, land or Sun glint masking. ECMWF wind fields at 850 mbar corresponding to an altitude of about 1.5 km are also plotted on the

a) 18–28 February 1999

b) 1–10 March 1999

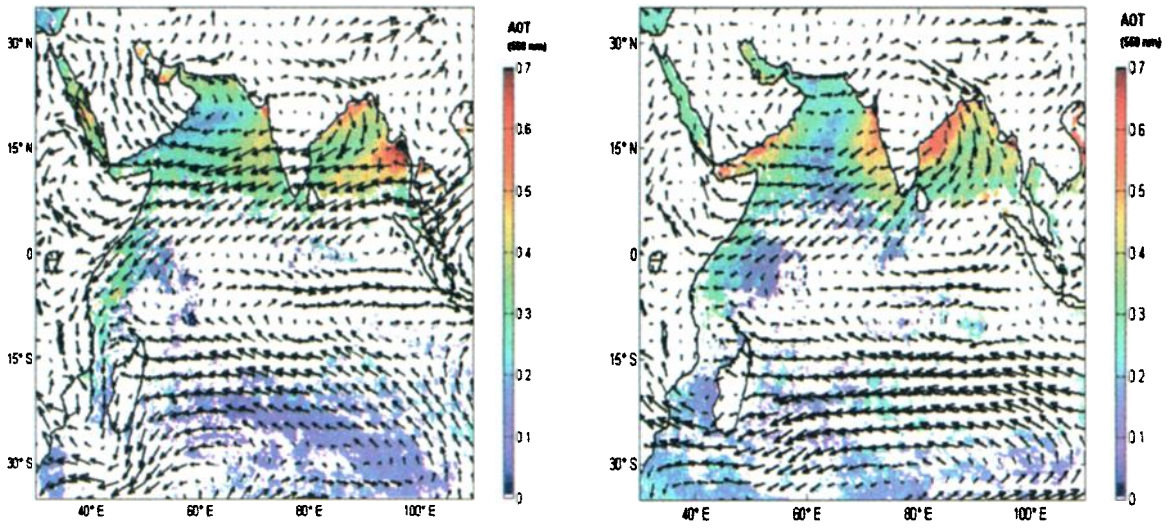

c) 11–20 March 1999

d) 21–30 March 1999

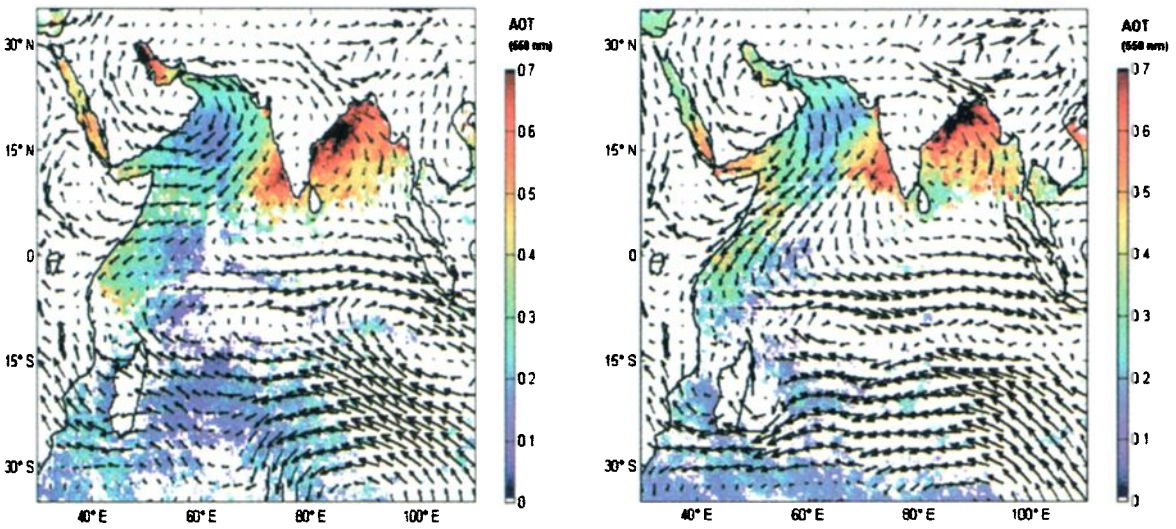

Plate 5. Mean Meteosat-5 derived AOT for (a) the last 10 days of February 1998, (b) the first, (c) the second and (d) the third period of 10 days of March 1999.

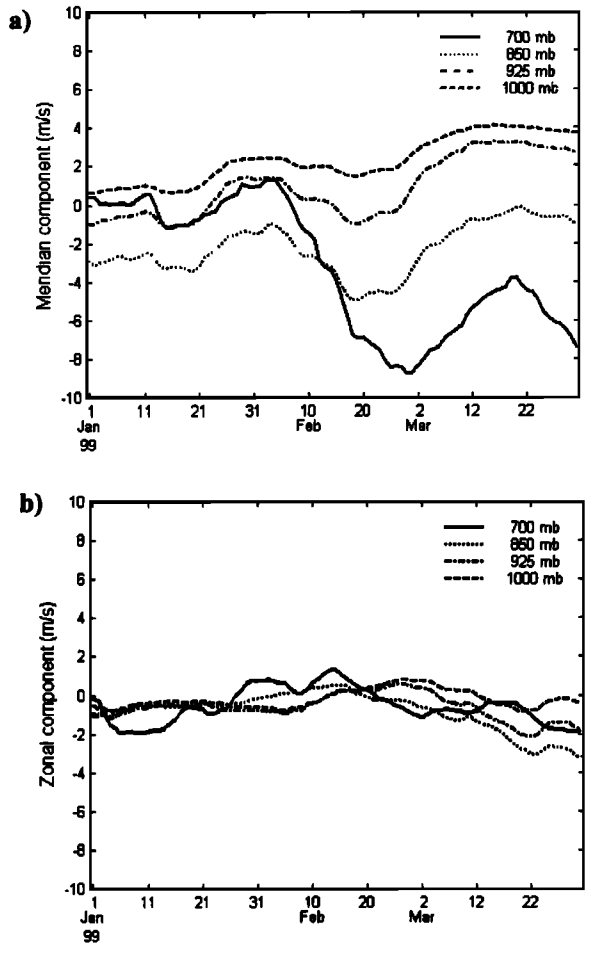

Figure 4. ECMWF (a) meridian wind component and (b) zonal wind component plotted for level 1000 mbar, 925 mbar, 850 mbar and 700 mbar at the location of the Goa experimental site as a function of the day. Positive values correspond to the north direction for the meridian wind component and to the west direction for the zonal wind component.

plates. The regional extent of the aerosol plume during the last 10 days of February (Plate 5a) and the 10 first days of March (Figure 5b) is limited to the upper north of the Indian Ocean. During the second (Plate 5c) and the third (Plate 5d) period of 10 days, we can observed an increase in the AOT and in the geographical extent toward the south of the plumes spreading over the Arabian Sea and the Bay of Bengal.

During the second decade of March the Bay of Bengal is covered by a haze with AOT ranging from 0.9 close to Calcutta to 0.45 north of Sri-Lanka. Wind fields suggest that the plume over the Bay of Bengal and NIO originate from the Ganges Valley and from southern India, respectively, and may be transported toward the Intertropical Convergence Zone located between 0° and 10°S during the IFP.

4.2. Regional Transport

To identify origins of the observed aerosol plume, we have performed simulations using LMDZ.3.3. Back plumes arriving over the Goa station for February and March 1999 have been simulated for two levels: in the planetary boundary layer and in the monsoon layer at 2 km altitude. A main feature in the transport of polluted air masses to the ground-based station is that the aerosol plume has mainly a continental origin. A change appears in the planetary boundary layer between February when air masses comes from northeast of the Goa station and March when the station is mainly affected by air masses originating from the Bombay area. Indeed, as shown on Figure 4a, the ECMWF meridian wind component over the station is increasing continuously during the period. The difference of transport within the planetary boundary layer between the two periods could explain the decrease of BC concentration recorded at Goa.

The second difference observed is that during February air masses in the monsoon layer originate from the east while originate from the southeast in March. Figures 4a and 4b show that a change in the wind direction occurs specifically at the 700 mbar level. South India (Tamil Nadu and Sri Lanka) is an area of convection and plays a major role in the distribution of pollutants in the free troposphere in this region.

By use of the Model of Atmospheric Transport and Chemistry (MATCH model) combined with an assimilation package developed for applications in atmospheric chemistry [*Collins et al.*, 2001], *Rasch et al.* [2001] describe the outflow of aerosol originating from the Bay of Bengal to the Maldives and South India. During the second half of the IFP they found that the southward plume from Bombay is confined to the planetary boundary layer, and is weaker than during the first half. This is in agreement with the decrease of the BC concentration that we recorded near the ground at Goa (Plate 2d). They also found an enhancement of the westward flow off the southwest coast of India corresponding to an enhancement of the offshore transport of aerosols at 2.5 km. Our analysis confirms those simulations.

It has to be noted that the growth of the aerosol load in the monsoon layer may not only be due to a change in the atmospheric circulation but could also be linked to an increase in source intensity. Soot is one of the major constituent of the aerosol in the NIO [*Satheesh and Ramanathan*, 2000; *Ramanathan et al.*, this issue]. Soot particles are originating from fossil fuel consumption and biomass burning [*Penner et al.*, 1991]. Industrial and traffic emission have a weak seasonal variability. An hypothesis for the increase in AOT over Arabian Sea as well as over the Bay of Bengal may be an increase in biomass burning emissions. To check this hypothesis, we have analyzed ATSR Fire Product [*Arino*, 1997]. Figure 5 displays the number of fires observed in India (area 8°-35°N, 70°-90°E) over the dry period (November 1998 to May 1999). Over India the monthly average number of fires has been multiplied by a factor of 1.7 between January and February and further multiplied by 5.2 between February and March. The correlation

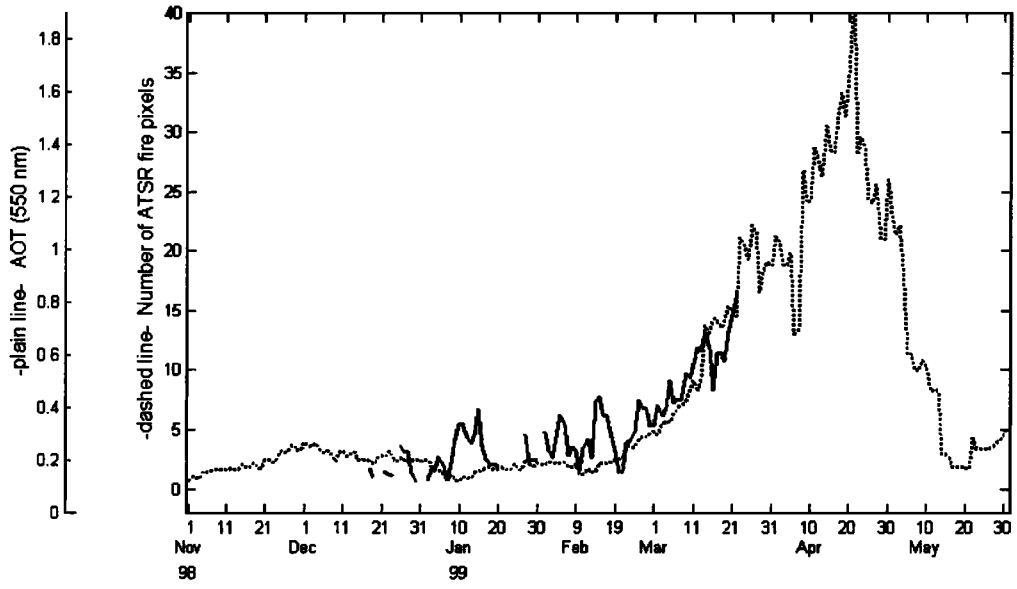

Figure 5. Moving average over 15 days of the number of fire detected by ATSR in India (area 8°-35°N, 70°-90°E). Data are available at http://shark1.esrin.esa.it/ionia/FIRE/.

with the AOT trend (also reported in Figure 5 for Dharwar) indicates that the increase in biomass burning in India is at least partly responsible of the AOT observed in the NIO.

4.3. Dust Event

In the previous section we have mainly focused on the interpretation of the change in the aerosol load between February and March. This attention was motivated by analysis of Sun photometer derived AOT and AE. Indeed, those observations point out the trend in AOT over the IFP and the nearly constant value of the AE which suggest a constant spectral dependency of the aerosols inside the plume. Further analysis shows that at the end of the IFP (March 17-26), a special event was observed with a decrease in AOT from 0.7 to 0.3 and a decrease in AE from 1.4 to 0.9. We have reported on Plate 6, AOT image derived from Meteosat-5 analysis and the ECMWF wind field at 850 mbar on March 25. The image shows that an aerosol event has occurred in the Persian and Oman Gulfs and reaching the North of India on March 25. This region is well-known to be affected by transport of desert dust particles coming from Arabian and Middle East deserts [*Sirocko and Sarthein*, 1989; *Ackerman and Chung*, 1992]. The decrease in AE observed at Goa, characteristic of a mix-

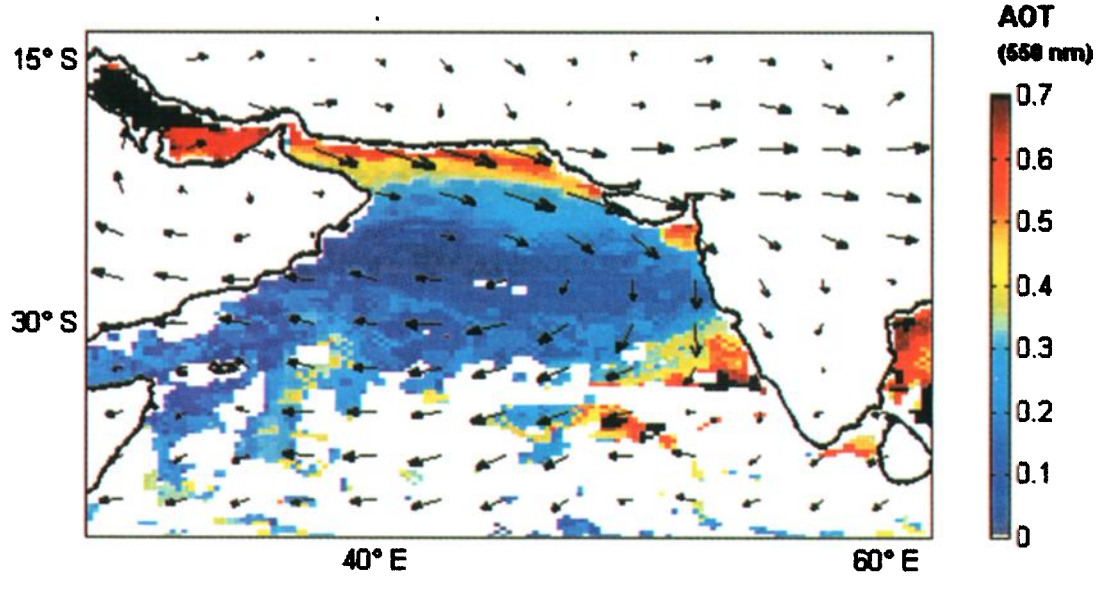

Plate 6. Meteosat-5 derived AOT on March 25, 1999. ECMWF wind direction and intensity at 850 mbar are also displayed.

ing between pollution aerosols and dust particles [*Hamonou et al.*, 1999], is associated with a decrease in AOT likely due to a shift of the monsoon turbid plume south of the ground-based station. Indeed, satellite imagery and wind fields (Plate 5) show that in a case of air mass advection from the northern Arabian Sea to the western coast of India, which is predominant in the second decade of March (Figure 5c), the pollution plume exported to the NIO is shifted southward compared to the situation prevailing in late February (Figure 5a) and early March (Figure 5b) when air masses are advected from the east.

5. Summary and Conclusion

In the frame of the intensive field phase of INDOEX, a set of instruments with aerosol measurement capabilities have been set up at a coastal site (Goa University, Goa) and an inland site (Dharwar, Karnataka University) in India. In this paper, in situ sampling of BC, columnar integrated (AOT) and vertically resolved (aerosol extinction coefficient profiles) measurements have been presented. Local-scale investigations point out that the columnar AOT increases significantly over both sites during March compared to January and February. Aerosol vertical extinction coefficients derived by lidar sounding show that this feature is linked to an increase in the aerosol extinction coefficient inside the monsoon layer above the planetary boundary layer. The atmospheric circulation is described between the two sites by use of mesoscale 3-D model simulations showing land-sea breeze as well as topographic effects. Those simulations show that pollutants are vertically distributed over the marine boundary layer due to advection of air masses from the Deccan Plateau over the Western Ghats.

The regional-scale advection of polluted air masses from India over the NIO has been observed using AOT derived from measurements performed in the visible channel of Meteosat. Those measurements confirm the increase in AOT in March compared to January and February and show the regional spatial extent of the well-defined aerosol plume which spread over the Arabian Sea to the Intertropical Convergence Zone. The conclusions presented in this paper regarding the advection of pollution from India should correspond to a general case during the winter monsoon as this period is characterized by a northeasterly predominant wind flow. Nevertheless, we present in the last section an event of dust aerosols following advection of air masses from the northwest Arabian Sea. Indeed, some perturbations occur in this predominant wintertime circulation which can affect the advection of aerosols from India.

This paper confirms that the long range transport of continental pollution from India to the NIO results from the advection of turbid air masses in a well-identified monsoon layer over the marine boundary layer. It highlights the importance of the coastal atmospheric circulation in the vertical distribution of pollutants. Moreover, it is suggested that the increase in biomass burning plays a significant role in the increasing trend in AOT during the winter dry monsoon season.

Acknowledgments. This work was sponsored by INSU/CNRS "Programme National de Chimie Atmosphérique" and "Programme National Atmosphere Ocean à multi-échelles." We acknowledge EUMETSAT which moved Meteosat-5 and provided the data freely. LMD/IPSL is acknowledged for providing the database with formatted Meteosat-5 visible channel data and ECMWF data. ATSR World Fire Atlas European Space Agency - ESA/ESRIN is acknowledged for ASTR fire product. The authors thank Gilles Bergametti for helpful discussion.

This is the LSCE contribution 0519.

References

Ackerman, S.A., and H. Chung, Radiative effects of airborne dust on regional energy budgets at the top of the atmosphere, *J. Appl. Meteorol.*, *31*, 223-233, 1992.

Andreae, M.O., and P.J. Crutzen, Atmospheric aerosols: Biogeochemical sources and role in atmospheric chemistry, *Science*, *276*, 1052-1058, 1997.

Angström, A., The parameters of atmospherics turbidity, *Tellus*, *16*, 64-75, 1964.

Arino, O., Regional satellite fire data compilation, Int. Geosphere-Biosphere Program Data and Inf. Syst., Toulouse, France, 1997.

Boucher, O., and T.L. Anderson, GCM assesment of the sensitivity of direct climate forcing by anthropogenic sulphate aerosol size and chemistry, *J. Geophys. Res.*, *100*, 26,117-26,134, 1995.

Charlson, R.J., S.E. Schwartz, J.M. Hales, R.D. Cess, J. J. A. Coakley, J.E. Hansen, and D.J. Hofmann, Climate forcing by anthropogenic aerosols, *Science*, *255*, 423-430, 1992.

Chazette, P., C. David, J. Lefrère, S. Godin, J. Pelon, and G. Mégie, Comparative lidar study of the optical, geometrical, and dynamical properties of stratospheric post-volcanic aerosols, following the eruptions of El Chichon and Mount Pinatubo, *J. Geophys. Res.*, *100*, 23,195-23,207, 1995.

Chazette, P., J.-F. Leon, H. Cachier, F. Dulac, S.C. Alfaro, L. Gomes, A. Gaudichet, J.-L. Rajot, J.G. Won, and S.C. Yoon, Consistence between lidar and ground-based measurements in the frame of INDOEX intensive field phase, *paper presented at 20th International Laser Radar Conference*, July 10-14, Vichy, France, 2000.

Coakley, J.A.J., et al., General overview of INDOEX, *J. Geophys. Res.*, in press, 2001.

Collins, W.D., P.J. Rasch, B.E. Eaton, B. Khattatov, J.-F. Lamarque, and C.S. Zender, Simulating aerosols using a chemical transport model with assimilation of satellite aerosol retrievals: Methodology for INDOEX, *J. Geophys. Res.*, *106*, 7313-7336, 2001.

Deuzé, J.L., M. Herman, P. Goloub, D. Tanré, and A. Marchand, Characterization of aerosols over the ocean from POLDER/ADEOS-1, *Geophys. Res. Lett.*, *26*, 1421-1424, 1999.

Dickerson, R.R., S. Kondragunta, G. Stenchikov, K.L. Civerolo, B.G. Doddridge, and B.N. Holben, The impact of aerosols on solar ultraviolet radiation and photochemical smog, *Science*, *278*, 827-830, 1997.

Fouquart, Y., B. Bonnel, M.C. Roquai, R. Santer, and A. Cerf, Observations of Saharan aerosols: Results of

ECLATS field experiment, part I, Optical thicknesses and aerosol size distributions, *J. Clim. Appl. Meteorol.*, *26*, 28-37, 1987.

Govaerts, Y.M., B. Pinty, M.M. Verstraete, and J. Schmetz, Exploitation of angular signature to calibrate geostationary satellite solar channels, *paper presented at the International Geoscience And Remote Sensing Symposium*, Seattle, Wash., 1998.

Hamonou, E., P. Chazette, D. Balis, F. Dulac, X. Schneider, E. Galani, G. Ancellet, and A. Papayannis, Characterisation of the vertical structure of Saharan dust export to the Mediterranean basin, *J. Geophys. Res.*, *104*, 22,257-22,270, 1999.

Herman, B.M., M.A. Box, J.A. Reagan, and C.M. Evans, Alternate approach to the analysis of solar photometer data, *Appl. Opt.*, *20*, 2925-2928, 1981.

Hess, P., N. Srimani, and S. Flocke, Trajectories and related variations in the chemical composition of air for the Mauna Loa observatory during 1991 and 1992, *J. Geophys. Res.*, *101*, 14,543-14,568, 1996.

Holben, et al., AERONET-A federated instrument network and data archive for aerosol characterisation, *Remote Sens. Environ.*, *66*, 1-16, 1998.

Hourdin, F., and J.P. Issartel, Reciprocity of atmospheric transport of trace species., *C. R. Acad. Sci.*, *329*, 623-628, 2000.

Intergovernmental Panel on Climate Change (IPCC), Climate Change 1995, *Cambridge Univ. Press*, New York, 1995.

Jayaraman, A., D. Lubin, S. Ramachandran, V. Ramanathan, E. Woodbridge, W.D. Collins, and Z.S. Zalpuri, Direct observations of aerosol radiative forcing over the tropical Indian Ocean during the January-February 1996 pre-INDOEX cruise, *J. Geophys. Res.*, *103*, 13,827-13,836, 1998.

Kikuchi, Y., S. Arakawa, F. Kimura, K. Shirasaki, and Y. Nagano, Numerical study on the effects of mountains on the land sea breeze circulation in the Kanto district, *J. Meteorol. Soc. Jpn.*, *59*, 723-737, 1981.

Klett, J.D., Lidar calibration and extinction coefficients, *Appl. Opt.*, *22*, 514-515, 1983.

Liousse, C., C. Devaux, F. Dulac, and H. Cachier, Aging of savanna biomass burning aerosols: Consequences on their optical properties., *J. Atmos. Chem.*, *22*, 1-17, 1995.

Mahrer, Y., and R.A. Pielke, A test of an upstream spline interpolation technique for the advective terms in a numerical mesoscale model, *Mon. Weather Rev.*, *106*, 818-830, 1978.

Moorthy, K.K., S.K. Sateesh, and B.V. Krishna Murthy, Characteristics of spectral optical depths and size distributions of aerosols over the tropical oceanic regions, *J. Atmos. Sol. Terr. Phys.*, *60*, 981-992, 1998.

Moulin, C., F. Dulac, C.E. Lambert, P. Chazette, I. Jankowiak, B. Chatenet, and F. Lavenu, Long-term daily monitoring of Saharan dust load over ocean using ISCCP-B2 data, 2, Accuracy of the method and validation using Sun photometer measurements, *J. Geophys. Res.*, *102*, 16,959-16,969, 1997a.

Moulin, C., F. Guillard, F. Dulac, and C.E. Lambert, Long-term daily monitoring of Saharan dust load over ocean using ISCCP-B2 data, 1, Methodology and preliminary results for 1983-1994 in the Mediterranean, *J. Geophys. Res.*, *102*, 16,947-16,958, 1997b.

Ookouchi, Y., and Y. Wakata, Numerical simulation for the topographical effect on the sea-land breeze in the Kyushu island, *J. Meteorol. Soc. Jpn.*, *62*, 864-879, 1984.

Pelon, J., P.H. Flamant, and M. Meisonnier, The french airborne backscatter lidar Leandre-1: conception and operation, *paper presented at the 15th International Laser Radar Conference*, Tomsk, Russia, 1990.

Penner, J.E., Carbonaceous aerosols influencing atmospheric radiation: Black and organic carbon, in *Report of the Dahlem Workshop on Aerosol Forcing of Climate*, edited by R.J. Charlson and J. Heintzenberg, pp. 91-108, John Wiley, New York, 1995.

Penner, J.E., S.J. Ghan, and J.J. Walton, The role of biomass burning in the budget and cycle of carbonaceous soot aerosols and their climate impact, in *Global Biomass Burning*, edited by J.S. Levine, MIT Press, Cambridge, Mass., 1991.

Ramanathan, V., et al., *Indian Ocean Experiment (INDOEX) white paper*, Univ. of Calif., San Diego, 1995.

Ramanathan, V., et al., Indian Ocean Experiment: An integrated analysis of the climate forcing and effects of the great Indo-Asian haze, *J. Geophys. Res.*, this issue.

Rasch, P.J., W.D. Collins, and B.E. Easton, Understanding the Indian Ocean Experiment (INDOEX) aerosol distributions with an aerosol assimilation, *J. Geophys. Res.*,*106*,7337-7355, 2001.

Ruellan, S., and H. Cachier, Characterization of fresh particular exhausts near a Paris high flow road, *Atmos. Environ.*, *35*, 453-458, 2001.

Satheesh, S.K., and V. Ramanathan, Large difference in tropical aerosol forcing at the top of the atmosphere and Earth's surface, *Nature*, *405*, 60-63, 2000.

Satheesh, S.K., K. Krishna Moorthy, and B.V. Krishna Murthy, Spatial gradients in the aerosol characteristics over the Arabian Sea and Indian Ocean, *J. Geophys. Res.*, *103*, 26,183-26,192, 1998.

Sirocko, F., and M. Sarthein, Wind-borne deposits in the northwestern Indian Ocean: Record of Holocene sediments versus modern satellite data, in *Paleoclimatology and Paleometeorology: Modern and Past Patterns of Global Atmospheric Transport*, edited by M. Leinen and M. Sarnthein, pp. 401-433, Kluwer Acad. Norwell, Mass., 1989.

Spinhirne, J.D., Micro pulse lidar, *IEEE Trans. Geosci. Remote Sens.*, *31*, 48-55, 1993.

Tanré, D., C. Devaux, M. Herman, and R. Santer, Radiative properties of desert aerosols by optical ground-based measurements at solar wavelengths, *J. Geophys. Res.*, *93*, 14,223-14,231, 1988.

Twomey, S.A., Pollution and the planetary albedo, *Atmos. Environ.*, *8*, 1251-1256, 1974.

Warneck, P., *Chemistry of the Natural Atmosphere*, Academic, San Diego, Calif., 1988.

S. C. Alfaro, A. Gaudichet, L. Gomes and J.-L. Rajot, LISA, CNRS-Université PVII/PXII, 94010 Créteil, France.

M. Bonazzola, LMD, CNRS, 75252 Paris, France.

H. Cachier, P. Chazette, F. Dulac, E. Hamonou and J.-F. Leon, LSCE, CEA-CNRS, 91191 Gif-sur-Yvette, France. (email: leon@loa.univ-lille1.fr).

S. Cautenet and G. Foret, LaMP, CNRS-Université Blaise Pascal, 63000, Clermont-Ferrand, France.

C. Flamant and J. Pelon, SA, CNRS, 75252 Paris, France.

S. R. Inamdar and J. S. Kadadevarmath, Department of Physics, Karnataka University, Dharwar 580 003, Karnataka, India.

F. Lavenu, CESBIO, CNES, 31401 Toulouse, France.

P. R. Sarode, Department of Physics, Goa University, Taleigo plateau 403 206, Goa, India.

(Received August 15, 2000; revised November 30, 2000; accepted January 11, 2001.)